

# Zero-Dark-Counting Brief Measurement of X-ray Spectra Using a Lutetium-Oxyorthosilicate Multipixel-Photon Detector Driven in Pre-Geiger Mode

Toshiyuki Enomoto<sup>1</sup>, Eiichi Sato<sup>2</sup>, Hodaka Moriyama<sup>3</sup>, Osahiko Hagiwara<sup>4</sup>, Hiroshi Matsukiyo<sup>5</sup>, Manabu Watanabe<sup>6</sup>, Shinya Kusachi<sup>7</sup>

<sup>1, 3, 4, 5, 6, 7</sup>Department of Surgery, Toho University Ohashi Medical Center, 2-17-6 Ohashi, Meguro, Tokyo, Japan

<sup>2</sup>Department of Physics, Iwate Medical University, 2-1-1 Nishitokuta, Yahaba, Iwate, Japan

**Abstract:** Brief measurement of X-ray spectra using a detector, consisting of a lutetium oxyorthosilicate (LSO) crystal and a multipixel photon counter (MPPC) is described. X-ray photons are detected using the LSO crystal and a 0.5-mm-diam 3.0-mm-thick lead pinhole, and scintillation photons produced in the crystal are detected using the MPPC. The photocurrents flowing through the MPPC are converted into voltages and amplified using a stable high-speed current-voltage amplifier, and the output event pulses from the amplifier are sent to a multichannel analyzer to perform pulse-height analysis. Without the counts of  $\gamma$  photons from the LSO crystal, the dark count rate was reduced to 0 count per second by reducing the MPPC bias voltage to 65.11 V in the pre-Geiger mode. The photon energy was determined by two-point calibration using  $K\alpha$ -fluorescent energies of iodine and lead, and the energy resolutions was below 30% at 74.2 keV. Using the LSO-MPPC detector, both the maximum-photon and the peak-count energies increased with increasing tube voltage, and the maximum count rate was 31 kilocounts per second at a tube voltage of 100 kV and a current of 0.16 mA. Dual-energy computed tomography was accomplished using gadolinium contrast media.

**Keywords:** X-ray spectra; LSO-MPPC detector; pre-Geiger mode; stable I-V amplifier; zero dark counting; fluorescent energy calibration; dual-energy CT

## 1. Introduction

Currently, X-ray spectra are measured using a high-energy-resolution cadmium telluride (CdTe) detector, and the energy resolution has been improved to approximately 1% at 122 keV [1]. Therefore, we performed fundamental studies on photon-counting energy-dispersive computed tomography (ED-CT) scanners [2, 3] using CdTe detectors. Using these first-generation scanners, we carried out K-edge CT using iodine (I) and gadolinium (Gd) contrast media.

Recently, CdTe array detectors have been developed and applied in preclinical ED-CT scanners [4-6] to perform K-edge CT. Therefore, we are constructing an ED-CT scanner with a dual-energy (DE) array detector [7] with pixel dimensions of  $0.1 \times 0.1 \text{ mm}^2$  to reduce the exposure time for CT and to perform 3D imaging. The exposure time for CT can be reduced, and the energy resolution of the array detector will be improved in the near future.

Compared with the CdTe detector, the X-ray photon count rate can be increased easily beyond 1 megacounts per second using scintillation detectors [8] consisting of a multipixel photon counter (MPPC) and a short-decay-time scintillation crystal. Without a lead (Pb) pinhole, the energy resolution of a lutetium-oxyorthosilicate (LSO) MPPC detector was 53% at 59.5 keV [9]. Lately, the bias voltage of the MPPC detector has been reduced, and the energy resolution of the LSO-MPPC detector can be improved using a pinhole. Therefore, we are interested in the application of the

LSO-MPPC detector to photon-counting DE-CT. Since the count rate can be increased utilizing the first-generation DE-CT, the image quality improves, and the exposure time for CT can be reduced.

The X-ray photon energy is calibrated using  $\gamma$  photons from standard radioisotopes (RIs). The energy resolution tends to improve with decreasing pinhole diameter attached to the LSO crystal, and it is difficult to increase the count rate of RIs using a small-diam pinhole. In this regard, the brief energy calibration using fluorescent  $K\alpha$  photons is useful for roughly determining both the energy and the energy resolution.

In our research, major objectives are as follows: to construct an LSO-MPPC detector with a pinhole, to improve a high-speed current-voltage (I-V) amplifier, to roughly determine the photon energy without standard RIs, to measure X-ray spectra with high count rates, and to confirm imaging effect using a DE counter [10] with the detector. Therefore, we measured the X-ray spectra using the LSO-MPPC detector and performed first-generation DE-CT using Gd media.

## 2. Experimental Setup

### 2.1 Measurement of X-Ray Dose Rate

The measurement of X-ray dose rate is important to calculate incident dose for objects. To measure the dose rate from an X-ray generator, we used an ionization chamber (RAMTEC 1000 plus, Toyo Medic) placed 1.0 m from the X-ray source at

a constant tube current of 0.16 mA without filtration.

## 2.2 Measurement of X-Ray Spectra Using CdTe

X-ray spectra for reference were measured using a readily available CdTe detector system (XR-100T, Amptek). In this system, a CdTe is fixed directly to the charge-sensitive amplifier, and the outputs are input to a shaping amplifier. The event pulses from the shaping amplifier are sent to a multichannel analyzer (MCA; MCA 4000,  $\gamma$ PGT) to perform pulse-height analysis. The X-ray spectra were observed on the monitor of a personal computer (PC). The photon energy was determined by two-point calibration using  $K\alpha_1$  fluorescence of I and Pb.

## 2.3 Measurement of Spectra Using LSO-MPPC

Figure 1 shows the experimental setup for measuring X-ray spectra using an LSO-MPPC (S12572-100C, Hamamatsu) detector. X-ray photons passing through a 0.5-mm-diam 3.0-mm-thick Pb pinhole are detected by the LSO single crystal with a decay time of 40 ns, and the scintillation photons are detected by the MPPC with an effective photosensitive dimensions of  $3.0 \times 3.0 \text{ mm}^2$ . The dimensions of the LSO crystal are  $2.5 \times 2.5 \times 1.0 \text{ mm}^3$ , and the crystal is stuck on the photosensitive surface using an epoxy-resin adhesive. The bias voltage of the MPPC is 65.11 V in the pre-Geiger mode, and photocurrents flowing through the MPPC are converted into voltage and amplified using an I-V amplifier at a constant temperature of 22°C. The 100-ns-width event pulses from the amplifier are input to the MCA to measure X-ray spectra.

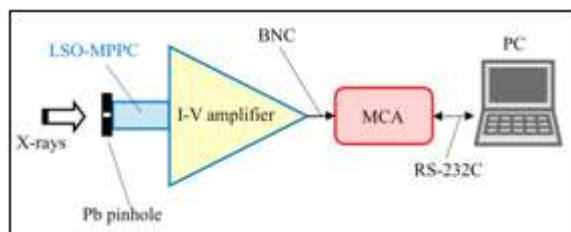
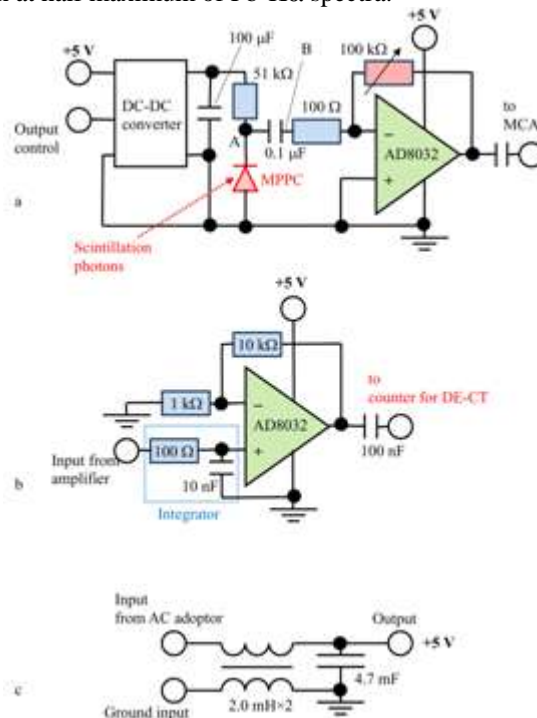


**Figure 1:** Block diagram for measuring X-ray spectra using an LSO-MPPC detector, a high-speed I-V amplifier, and an MCA at a tube current of 0.16 mA. A 0.5-mm-diam 3.0-mm-thick Pb pinhole is used to improve the energy and spatial resolutions of DE-CT.

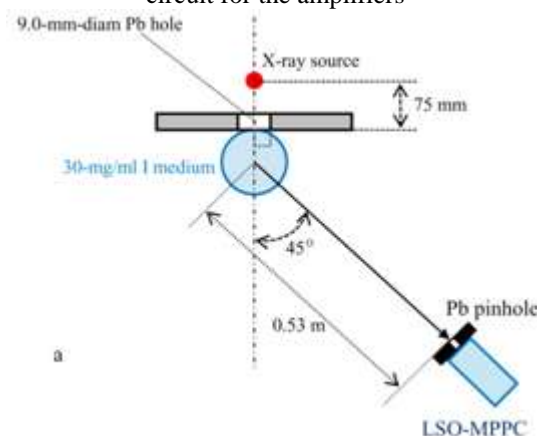
The circuit diagram of the high-speed I-V amplifier is shown in Fig. 2. When the photocurrents flow, the electric potential at a point A decreases, and the negative pulse produced at a point B is amplified by the high-speed inverse-amplifying circuit using an 80 MHz band-width operational amplifier (AD8032, Analog Devices) [Fig. 2(a)]. To detect peak-event voltages correctly using the MCA, the event-pulse width is increased using a 1- $\mu$ s-constant integrator, and the peak voltage is amplified using a simple amplifier [Fig. 2(b)]. A smoothing circuit with a common-mode inductor and a 4.7-mF condenser are useful for reducing electric noises from the amplifiers [Fig. 2(c)].

The photon energy was determined by two-point calibration using  $K\alpha$  fluorescent photons of I and Pb. The experimental

arrangements for detecting  $K\alpha$  photons are shown in Fig. 3. A 9.0-mm-diam Pb diaphragm was used to reduce the X-ray exposure field. The quasi-monochromatic I-K photons from a 15-mm-diam glass vial filled with 30-mg/ml I medium are detected by the LSO-MPPC detector with the pinhole in the direction with an angle of  $45^\circ$  from the X-ray axis to avoid direct photons from the X-ray source [Fig. 3(a)]. The Pb pinhole was used to improve the energy resolution and to measure spectra for the first-generation DE-CT. The tube voltage was 60 kV, and the tube current was increased to 1.0 mA to increase the count rate of I fluorescence. To detect Pb  $K\alpha$  photons, a 0.3-mm-thick Pb plate was used [Fig. 3(b)], the tube current was 1.0 mA, and the tube voltage was increased to 109 kV to excite Pb atoms. The energy resolution of the LSO-MPPC detector was roughly determined by the half width at half maximum of Pb- $K\alpha$  spectra.



**Figure 2:** Circuit diagrams of the I-V amplifier for the MPPC. (a) Inverse high-speed I-V amplifier for converting photocurrents into event-output voltages, (b) 1- $\mu$ s integrator with a simple amplifier for the MCA, and (c) smoothing circuit for the amplifiers



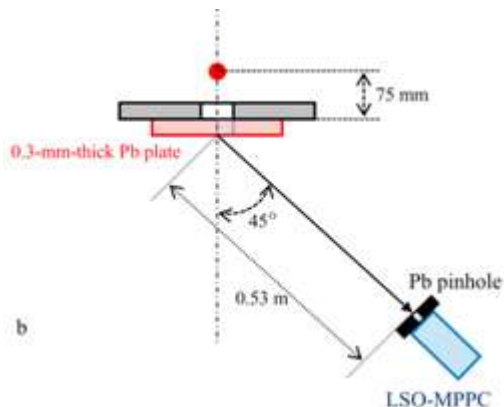


**Figure 3:** Experimental arrangement for measuring K fluorescence. (a) Method for measuring I fluorescence from a glass vial filled with I medium, and (b) method for measuring Pb fluorescence from the Pb plate. Quasi-monochromatic K photons are detected by the LSO-MPPC detector with the pinhole in the direction with an angle of 45° from the X-ray axis

### 2.4 DE-CT Scanner

Figure 4 shows an experimental setup of the DE-CT scanner. The distance between the X-ray source (RXG-0152, R-tec) and the detector set is 1.00 m, and the distance from the center of turntable (SGSP-60YAW-OB, Siguma Koki) to the detector set is 0.15 m to decrease the scattering photon counts from the object. To improve the spatial resolution, the 0.5-mm-diam pinhole is set in front of the LSO-MPPC detector.

In the scanner, both the X-ray source and the detector are fixed, and the object on the turntable oscillates on the scan stage (SGSP-26-100, Siguma Koki) with a velocity of 25 mm/s and a stroke of 60 mm. The X-ray projection curves for tomography are obtained by repeated linear scans and rotations of the object, and the scanning is conducted in both directions of its movement. Both the scan stage and turntable are driven by the two-stage controller (SHOT-602, Siguma Koki). Two step values of the linear scan and rotation are selected to be 0.5 mm and 1.0°, respectively. Using this CT scanner, the exposure time is 9.8 min at a total rotation angle of 180°. To perform DE-CT, we used a DE photon counter [10] with two energy selector (ESs). The event pulses from the I-V amplifier are input two ESs simultaneously, and two energy ranges for DE-CT are 10-50 and 50-100, respectively.

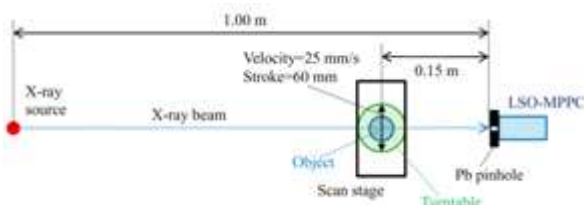


**Figure 4:** Experimental setup of the main components in the DE-CT scanner. The DE-CT is performed by repeated linear translations using an LSO-MPPC and rotations of the object.

## 3. Results

### 3.1 X-Ray Dose Rate

At a constant tube current of 0.16 mA, the X-ray dose rate increased with increasing tube voltage. At a tube voltage of 100 kV, the X-ray dose rate was 13.2  $\mu\text{Gy/s}$  at 1.0 m.

### 3.2 X-Ray Spectra Using CdTe

X-ray spectra measured using the CdTe detector with changes in the tube voltage are shown in Fig. 5. Gd K-edge energy of 50.2 keV is shown for reference to perform K-edge CT. Both the maximum-photon and bremsstrahlung-maximum-count energies increased with increasing tube voltage. At a tube voltage of 100 kV, sharp W-K lines were observed.

Figure 6 shows X-ray spectra for determining the photon energy measured using the CdTe detector. At a tube voltage of 60 kV, sharp I-K lines were observed, and  $K\beta$  counts are smaller than those of  $K\alpha$  [Fig. 6(a)]. Using the Pb plate, quasi-monochromatic K lines were selected out [Fig. 6(b)].

### 3.3 X-Ray Spectra Using LSO-MPPC

The X-ray spectra using the LSO-MPPC detector for determining the energy are shown in Fig. 7; these spectra correspond to those in Fig. 6. It was possible to roughly determine the energy, and the average energies of I- $K\alpha$  and Pb- $K\alpha$  are 28.5 and 74.2 keV respectively. Using Pb- $K\alpha$  lines, the energy resolution was below 30% at 74.2 keV with the pinhole.

Figure 8 shows X-ray spectra with changes in the tube voltage at a tube current of 0.16 mA. Both the maximum and maximum-count energies increased with increasing tube voltage. Compared with spectra in Fig. 5, the maximum-count energy at a tube voltage of 50 kV was almost equal, and the maximum-count energy shifted to high energies owing to the K-photon irradiation at tube voltages of 75 and 100 kV.

X-ray imaging is very easy to roughly confirm the ED effect of the detector. Therefore, we performed first-generation DE-CT at two energy ranges of 10-50 and 50-100 keV (Fig. 9). In particular, the range of 10-50 keV is useless for imaging Gd atoms [Fig. 9(a)], and the range of 50-100 keV is useful for carrying out Gd-K-edge CT [Fig. 9(b)].

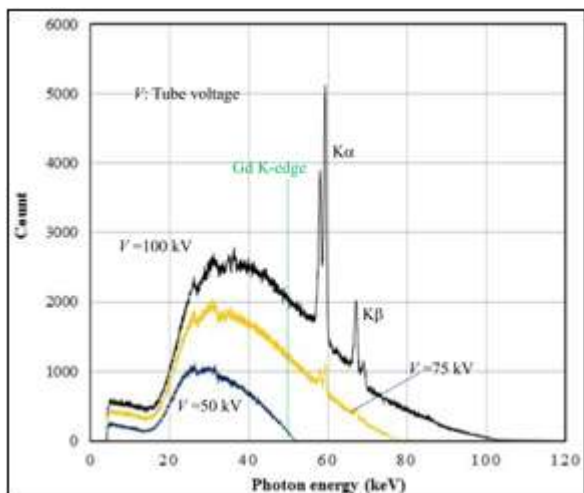


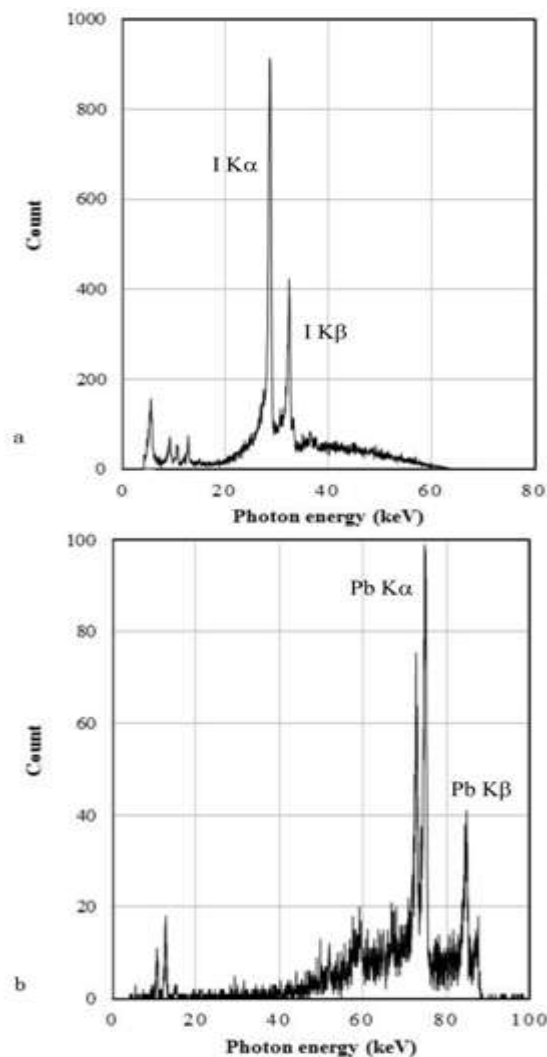
**Figure 5:** X-ray spectra for reference measured using the CdTe detector with changes in the tube voltage at a tube current of 12  $\mu$ A.

### 3.4 DE-CT

Tomography was performed at a constant tube voltage of 100 kV and a tube current of 0.16 mA. Tomograms are obtained as JPEG files, and the maximum and minimum gray-value densities are defined as white (255) and black (0), respectively.

Tomograms of two glass vials filled with two-different density Gd (meglumine gadopentetate) media of 15 and 30 mg/ml are shown in Fig. 10, and the density analysis of the tomograms using a program Image J is shown in the same figure. Using an energy range of 10-50 keV, the Gd-medium densities were quite lower than those of glass walls, and image-density difference between two media was small. Utilizing K-edge CT at an energy range of 50-100 keV, the Gd-medium densities substantially increased, and image-density difference was large. In addition, it was difficult to image glass walls, and the artifact between the vials were observed.

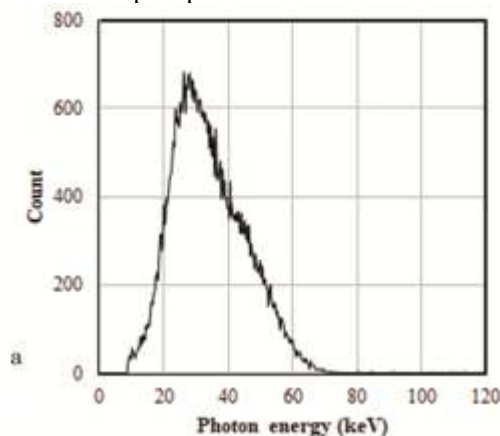
Figure 11 shows the result of the tomography of a rabbit-head phantom. The blood vessels were filled with gadolinium oxide ( $Gd_2O_3$ ) microparticles. Radiography (angiography) was performed for reference using a flat-panel detector (FPD; Rad-ikon Imaging 1024EV) to observe blood vessels. In radiography, fine blood vessels were observed with pixel dimensions of  $48 \times 48 \mu m^2$ . At a range of 10-50 keV, the densities of bone and muscle were high, and blood vessels were slightly observed. At a range of 50-100 keV, the bone and muscle density decreased, and thick vessels were visible at high contrasts.



**Figure 6:** X-ray spectra measured using the CdTe detector. (a) X-ray fluorescence from I medium at a tube voltage of 60 kV and (b) fluorescence from the 0.3-mm-thick Pb plate at a tube voltage of 109 kV.

### 4. Discussion

We measured X-ray spectra from a tungsten-target tube using an LSO-MPPC detector and an MCA at tube voltages below 100 kV and a current of 0.16 mA. In this regard, the maximum count rate of the LSO-MPPC detector was 31 kcps, and the rate can be increased easily to 100 kcps by increasing the tube current without the pileups.



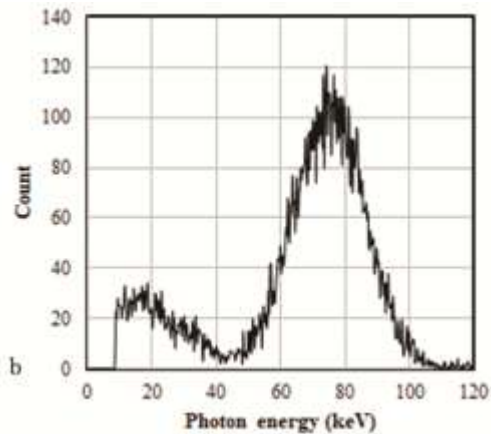


**Figure 7:** X-ray spectra measured using the LSO-MPPC detector. (a) Spectra from the I medium and (b) spectra from the 0.3-mm-thick Pb plate.

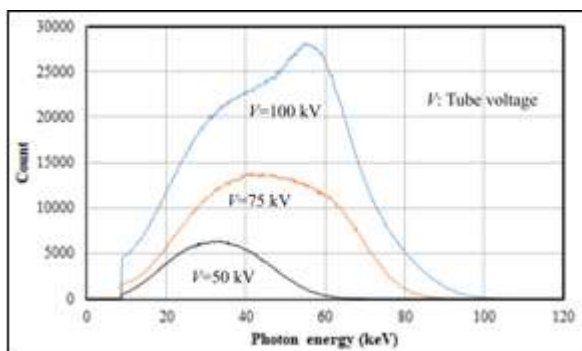


**Figure 8:** X-ray spectra measured using the LSO-MPPC detector with changes in the tube voltage at a tube current of 0.16 mA.

Currently, although the photon count of spectra substantially increases with decreasing photon energy using the LSO-MPPC detector in the Geiger mode owing to the dark counts, the X-ray spectra with energies ranging from 10 to 100 keV for biomedical diagnosis could be measured without dark counts by regulating the bias voltage to 65.11 V in the pre-Geiger mode. Compared with an LSO-MPPC with a photosensitive-surface dimensions of  $1.0 \times 1.0 \text{ mm}^2$ , the sensitivity of this detector with dimensions of  $3.0 \times 3.0 \text{ mm}^2$  was high. Thus, the bias voltage could be reduced, and the energy resolution was improved using a Pb pinhole at a constant temperature.

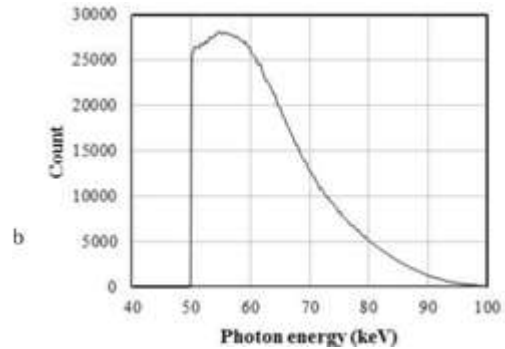
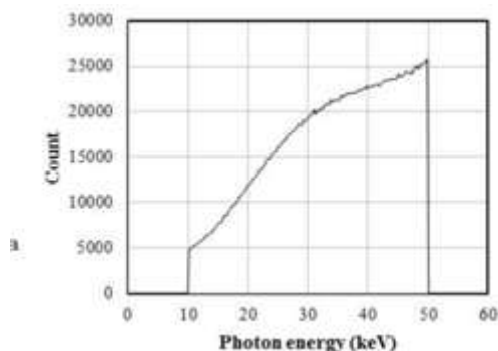


**Figure 9:** Selected X-ray spectra for DE-CT at a tube voltage of 100 kV. (a) X-ray photons at an energy range of 10-50 keV and (b) photons at a range of 50-100 keV for Gd-K-edge CT.

Brief energy determination for measuring X-ray spectra is important because optimal standard  $\gamma$ -ray sources are not necessary. Using the scintillation detectors, the energy resolution tends to improve with decreasing the pinhole diameter. However, it is quite difficult to increase the count rate of  $\gamma$  photons from the RI using the pinhole. In this regard, the two-point energy calibration using K-fluorescence photons of I and Pb is useful, since the elements of the X-ray shield and the X-ray contrast medium are Pb and I, respectively.

By considering the energy resolution, the first-generation DE-CT is suitable to roughly confirm the ED effect of the LSO-MPPC detector. Utilizing Gd-K-edge CT, the muscle and bone densities decreased, and blood vessels were observed at high contrasts. In this case, high-energy photons beyond 65 keV were also useful for decreasing muscle and bone densities without decreases in the vessel density.

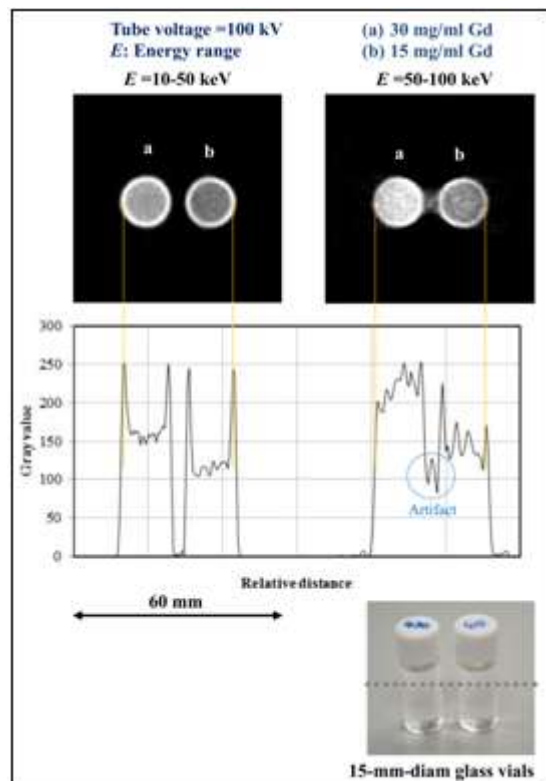


**Figure 10:** Tomograms of two glass vials filled with Gd media of two-different densities of 15 and 30 mg/ml. The densities of the Gd media were low, and the glass walls were

visible at a range of 10-50 keV. Both the Gd-medium densities and the density difference between two media substantially increased using Gd-K-edge CT at a range of 50-100 keV.

In the DE-CT, the maximum count per measuring point was approximately 0.6 kilocounts with a scan step of 0.5 mm and the scan velocity of 25 mm/s. The pixel dimensions of the reconstructed CT image were  $0.5 \times 0.5 \text{ mm}^2$  because the scan step was 0.5 mm. The original spatial resolution was primarily determined by the pinhole diameter of 0.5 mm, and the spatial resolutions were approximately  $0.5 \times 0.5 \text{ mm}^2$ .

## 5. Conclusions

We measured the X-ray spectra using an LSO-MPPC detector in conjunction with a high-speed I-V amplifier. The event-pulse widths were approximately 100 ns, and the energy resolution was below 30% at 74.2 keV using a 0.5-mm-diam Pb pinhole. The dark-count rate from the MPPC was reduced to 0 cps by decreasing the bias voltage. Thus, low-energy X-ray photons were detected, and the two tomograms with energy ranges below and beyond the Gd-K-edge energy were obtained simultaneously using Gd media.

## 6. Acknowledgments

This work was supported by Grants from Promotion and Mutual Aid Corporation for Private Schools of Japan, Japan Science and Technology Agency (JST), and JSPS KAKENHI (17K10371, 2017-2020). This was also supported by a Grant-in-Aid for Strategic Medical Science Research (S1491001, 2014–2018) from the Ministry of Education, Culture, Sports, Science and Technology of Japan.

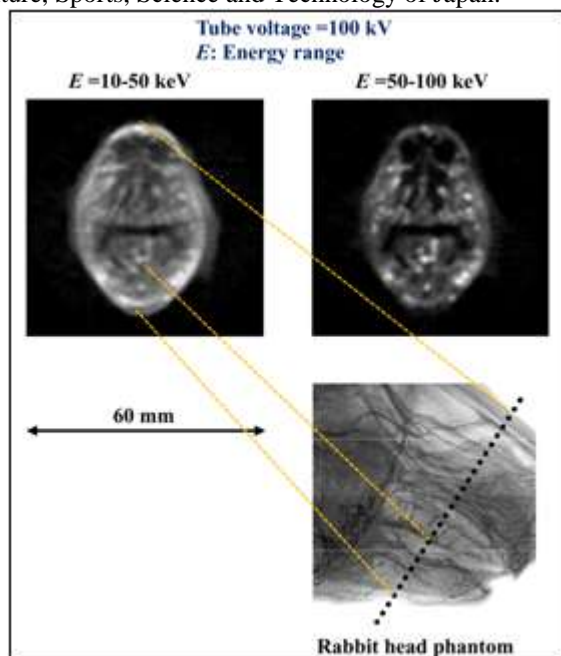


**Figure 11:** Tomograms of a rabbit-head phantom. Blood vessels were filled with  $\text{Gd}_2\text{O}_3$  microparticles. The densities of bone and muscle are high, and thick arteries were observed at low contrasts at a range of 10-50 keV. The muscle density decreased, and the image contrast of vessels improved at a range of 50-100 keV.

## References

- [1] Amptek US (2016). X-ray and  $\gamma$ -ray detector. <http://amptek.com/products/xr-100t-cdte-x-ray-and-gamma-ray-detector/>.
- [2] Hagiwara, O., Sato, E., Watanabe, M., Sato, Y., Oda, Y., Matsukiyo, H., Osawa, A., Enomoto, T., Kusachi, S., Ehara, S. (2014). Investigation of dual-energy X-ray photon counting using a cadmium telluride detector and two comparators and its application to photon-count energy subtraction. *Japanese Journal of Applied Physics*, 53, 102202-1-6.
- [3] Sato, E., Oda, Y., Abudurexiti, A., Hagiwara, O., Matsukiyo, H., Osawa, A., Enomoto, T., Watanabe, M., Kusachi, S., Sato, S., Ogawa, A., Onagawa, J. (2012). Demonstration of enhanced iodine K-edge imaging using an energy-dispersive X-ray computed tomography system with a 25 mm/s-scan linear cadmium telluride detector and a single comparator. *Applied Radiation and Isotopes*, 70, 831-836.
- [4] Feuerlein, S., Roessl, E., Proksa, R., Martens, G., Klass, O., Jeltsch, M., Rasche, V., Brambs, H.J., Hoffmann, M.H.K., Schlomka, J.P. (2008). Multienergy photon-counting K-edge imaging: potential for improved luminal depiction in vascular imaging. *Radiology*, 249, 1010-1016.
- [5] Ogawa, K., Kobayashi, T., Kaibuki, F., Yamakawa, T., Nanano, T., Hashimoto, D., Nagaoka, H. (2012). Development of an energy-binned photon-counting detector for X-ray and gamma-ray imaging. *Nuclear Instruments and Method in Physics Research Section A*, 664, 29-37.
- [6] Schlomka, J.P., Roessl, E., Dorscheid, R., Dill, S., Martens, G., Istel, T., Bäumer, C., Herrmann, C., Steadman, R., Zeitler, G., Livne, A. (2008). Experimental feasibility of multi-energy photon-counting K-edge imaging in pre-clinical computed tomography. *Physics in Medicine and Biology*, 53, 4031-4047.
- [7] Zscherpel, U., Walter, D., Redmer, B., Ewert, U., Ullberg, C., Weber, N., Pansar, T. (2014). Digital radiology with photon counting detectors. *Proceedings of 11th European Conference on Non-Destructive Testing, Prague*.
- [8] Sato, E., Sugimura, S., Endo, H., Oda, Y., Abudurexiti, A., Hagiwara, O., Osawa, A., Matsukiyo, H., Enomoto, T., Watanabe, M., Kusachi, S., Sato, S., Ogawa, A., Onagawa, J. (2012). 15 Mcps photon-counting X-ray computed tomography system using a ZnO-MPPC detector and its application to gadolinium imaging. *Applied Radiation and Isotopes*, 70, 336-340.
- [9] Yamaguchi, S., Sato, E., Oda, Y., Nakamura, R., Oikawa, H., Yabuushi, T., Ariga, H., Ehara, S. (2015). Measurement of X-ray spectra using a  $\text{Lu}_2(\text{SiO}_4)\text{O}$ -multipixel-photon detector with changes in the pixel number. *Applied Radiation and Isotopes*, 103, 25-30.
- [10] Sato, E., Kosuge, Y., Yamanome, H., Mikata, A., Miura, T., Oda, Y., Ishii, T., Hagiwara, O., Matsukiyo, H., Watanabe, M., Kusachi, S. (2017). Investigation of dual-energy X-ray photon counting using a cadmium telluride detector with dual-energy selection electronics. *Radiation Physics and Chemistry*, 130, 385-390.